

# The Effect of High Charging Rates Activation on the Specific Discharge Capacity and Efficiency of a Negative Electrode Based on a LaMgAlMnCoNi Alloy

E. A. Ferreira<sup>1,a</sup>; L. M. C. Zarpelon<sup>1,b</sup>; J. C. S. Casini<sup>1,c</sup>; H. Takiishi<sup>1,d</sup>  
and R. N. Faria<sup>1,e</sup>

<sup>1</sup> Energy and Nuclear Research Institute, IPEN/CNEN-SP, Av. Prof. Lineu Prestes, 2242, ZIP 05508-000, São Paulo, Brazil

<sup>a</sup>eaferrera@ipen.br, <sup>b</sup>zarpelon@ipen.br, <sup>c</sup>jasini@ipen.br, <sup>d</sup>takiishi@ipen.br; <sup>e</sup>rfaria@ipen.br

**Keywords:** Rare earth, Transition metal, Microanalyses, XRD, EDX.

**Abstract.** A nickel-metal hydride (Ni-MH) rechargeable battery has been prepared using a  $\text{La}_{0.7}\text{Mg}_{0.3}\text{Al}_{0.3}\text{Mn}_{0.4}\text{Co}_{0.5}\text{Ni}_{3.8}$  alloy as the negative electrode. The maximum discharge capacity of the  $\text{La}_{0.7}\text{Mg}_{0.3}\text{Al}_{0.3}\text{Mn}_{0.4}\text{Co}_{0.5}\text{Ni}_{3.8}$  alloy has been determined (350 mAh/g). Using a high starting charging rate ( $2857 \text{ mA g}^{-1}$ ) an efficiency of 49% has been achieved in the 4<sup>th</sup> cycle. The alloy and powders have been characterized by scanning electron microscopy (SEM), energy dispersive X-ray analysis (EDX) and X-ray diffraction (XRD).

## Introduction

Over the past years, LaNi-based hydrogen storage alloys for use in electrodes of rechargeable batteries have systematically incorporated specific alloying elements to improve the kinetics of hydrogen absorption and desorption, increase cycle life, improve corrosion resistance, etc. Cobalt, aluminum, manganese and magnesium are invariably present in the alloy composition [1-12]. Recently, it has been reported that, in the as-cast condition, a  $\text{La}_{0.7}\text{Mg}_{0.3}\text{Al}_{0.2}\text{Mn}_{0.1}\text{Co}_{0.75}\text{Ni}_{2.45}$  alloy electrode showed a maximum discharge capacity of 350.9 mAh/g with good cycling stability [13,14]. These studies were carried out using standard electrochemical impedance spectra (EIS), anode polarization and potential-step studies. In this study, a secondary battery has been produced using a  $\text{La}_{0.7}\text{Mg}_{0.3}\text{Al}_{0.3}\text{Mn}_{0.4}\text{Co}_{0.5}\text{Ni}_{3.8}$  alloy in the as-cast state and the maximum discharge capacity and the efficiency of the negative electrode has been determined. The influence of high charge rates on the electrode discharge activation and performance has been accessed.

## Experimental

A commercial alloy in the as-cast state was studied in this work. Ingots were prepared in a rectangular water-cooled copper mould in batches of approximately 5 kg. The as-cast microstructure of the starting alloy with a typical grain structure is shown in Fig. 1. The chemical analysis of the cast alloy is given in Table 1. For comparison convenience, a conversion to the substitution composition (atomic %) is also provided. Good agreement has been found between the composition specified values and that determined by analysis in the alloy. As per the supplier's specification, the alloys contain sulfur, oxygen and nitrogen as impurities (<10 ppm).

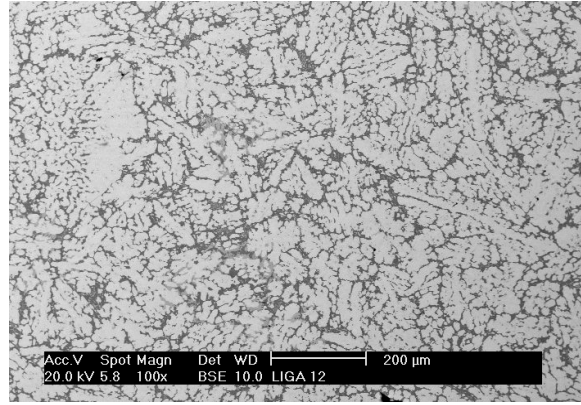


**Fig. 1** - Backscattered electron image of the as-cast microstructure of the  $\text{La}_{0.7}\text{Mg}_{0.3}\text{Al}_{0.3}\text{Mn}_{0.4}\text{Co}_{0.5}\text{Ni}_{3.8}$  alloy.

**Table 1.** Composition of the as-cast  $\text{La}_{0.7}\text{Mg}_{0.3}\text{Al}_{0.3}\text{Mn}_{0.4}\text{Co}_{0.5}\text{Ni}_{3.8}$  alloy.

Nominal composition and Substitution composition (at.%)	Specified and analyzed composition (wt.%)						
	La	Mg	Al	Mn	Co	Ni	C*
$\text{La}_{0.7}\text{Mg}_{0.3}\text{Al}_{0.3}\text{Mn}_{0.4}\text{Co}_{0.5}\text{Ni}_{3.8}$	25.12	1.88	2.09	5.68	7.61	57.62	--
$\text{La}_{11.67}\text{Mg}_5\text{Al}_5\text{Mn}_{6.67}\text{Co}_{8.33}\text{Ni}_{63.33}$	24.57	1.62	1.90	5.58	7.67	58.55	62

\*ppm (impurity)

In order to prepare the battery the following procedure was adopted. Five grams of the cast  $\text{La}_{0.7}\text{Mg}_{0.3}\text{Al}_{0.3}\text{Mn}_{0.4}\text{Co}_{0.5}\text{Ni}_{3.8}$  alloy was crushed with a mortar and pestle in air, such that all the material passed through a  $< 44 \mu\text{m}$  sieve. The powder (70 mg) was mixed with graphite and PTFE (50%) and pressed into a small electrode (approximately  $2 \times 2 \text{ cm}^2$ ; 1 mm thick). The battery was mounted and sealed in a square case using a commercial positive electrode ( $\text{NiOH}_2$ ) and separator. The specific discharge capacity was determined by discharging the battery at various charge and discharge rates. The hydrogen content of the charged electrode, expressed as the number of H atoms,  $n$ , per formula unit, was calculated from  $Q$  via the Faraday equation [3,4],

$$n = M_w Q / 26.8 \times 10^3 \quad (1)$$

where  $M_w$  is the molecular weight of the alloy ( $M_w=387.121 \text{ gmol}^{-1}$ ) and  $Q$  is in units of  $\text{mAhg}^{-1}$ . The efficiency of the alloy electrode was calculated using the ratio of discharge capacity to charge capacity. The battery properties measurements were carried out using a four channel computerized analyzer (Arbin-BT4).

Samples for the microstructure studies were prepared using conventional metallographic methods. The microstructures of the specimens were examined using a scanning electron microscope with energy dispersive X-ray analysis facility. Average data were obtained from various independent measurements from each phase.

## Results and Discussion

The chemical compositions of the phases, analyzed using EDX in the as-cast alloy, are presented in Table 2. The  $\text{La}_{0.7}\text{Mg}_{0.3}\text{Al}_{0.3}\text{Mn}_{0.4}\text{Co}_{0.5}\text{Ni}_{3.8}$  alloy is composed mainly of the matrix phase and two phases in the grain boundaries. Rare earth (RE) content in the matrix phase was about 15 at.%. Mg is below the EDX detection limit (assumed as 1 at.%) for this alloy. Al, Mn and Co are found inside the matrix phase which showed a RE:(Al, Mn, Co, Ni) atomic ratio of approximately 5, indicating a 1:5-type phase. Al-content in the gray phase (2.9 at.%) is lower but still close to that found for the matrix phase (3.9 at.%). Conversely, Mg-content in this phase is as high as 11 at.% whereas in the matrix phase stayed below the EDX detection limit. Mn-content (9.5

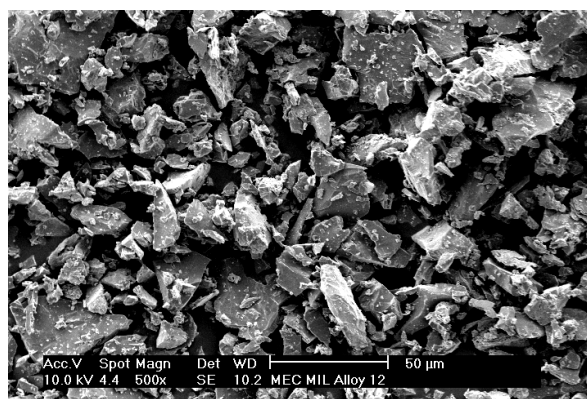
at.%) in the gray phase is three times as much that measured in the matrix phase (3.6 at.%). The chemical compositions of the dark phase showed that La-content was close or below to the EDX detection limit. EDX analyses also showed that this dark phase is very heterogeneous and the content of the main elements present (Mg, Al, Mn, Co, Ni) varied considerably.

**Table 2.** Composition determined by EDX at the centers of the matrix phase, the gray phase and the dark phase in the  $\text{La}_{0.7}\text{Mg}_{0.3}\text{Al}_{0.3}\text{Mn}_{0.4}\text{Co}_{0.5}\text{Ni}_{3.8}$  alloy.

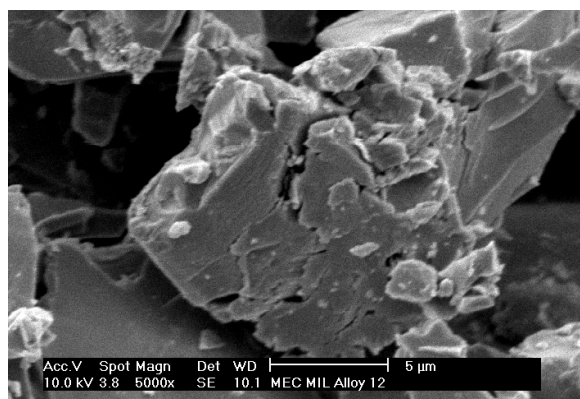
Phase	Analyzed composition (at.%)							N*
	La	Pr	Mg	Al	Mn	Co	Ni	
Matrix	15.4±0.6	-	<1	3.6±0.3	3.6±0.6	8.3±0.5	68.4±1.2	5
Gray	8.2±0.3	-	10.9±0.2	2.9±0.4	9.5±1.8	7.6±0.1	60.9±1.7	2
Dark	<1	-	1.8±0.2	9.5±0.4	15.1±0.1	16.2±0.3	56.8±0.2	3

\* Number of independent measurements from the matrix phase.

Secondary electron image of the powder prepared from the as-cast  $\text{La}_{0.7}\text{Mg}_{0.3}\text{Al}_{0.3}\text{Mn}_{0.4}\text{Co}_{0.5}\text{Ni}_{3.8}$  alloy is shown in Fig. 2a and 2b. This manually crushed material exhibits a wide size range of faceted grains, characteristic of this kind of milling. Fine grains as small as 5  $\mu\text{m}$  and, also, coarse grains as large as 50  $\mu\text{m}$  can be easily observed in this mechanically crushed material.



(a)



(b)

**Fig. 2 -** Secondary electron image of the powder prepared from the as-cast  $\text{La}_{0.7}\text{Mg}_{0.3}\text{Al}_{0.3}\text{Mn}_{0.4}\text{Co}_{0.5}\text{Ni}_{3.8}$  alloy (crushed with mortar and pestle; sieved < 44  $\mu\text{m}$ ): a) general view of the powder and b) details of the powder.

Charge capacity, discharge current density and specific discharge capacity for the Ni-MH battery prepared with a negative electrode using the  $\text{La}_{0.7}\text{Mg}_{0.3}\text{Al}_{0.3}\text{Mn}_{0.4}\text{Co}_{0.5}\text{Ni}_{3.8}$  alloy is given in Table 3. The electrode reached the maximum discharge capacity in the fourth cycle by using a high charging rate in the previous three cycles. The specific charge capacity plotted versus specific discharge capacity of the battery for cycles 3 to 8 is shown in Fig 4. Best charging capacity is 857  $\text{mAh/g}$ , which gave a maximum discharge capacity of 354  $\text{mAh/g}$ . The negative electrode, produced with a  $\text{La}_{0.7}\text{Mg}_{0.3}\text{Al}_{0.3}\text{Mn}_{0.4}\text{Co}_{0.5}\text{Ni}_{3.8}$  cast alloy, exhibited an excellent performance and a maximum discharge capacity of 354  $\text{mAh/g}$  (at a discharge density of 173  $\text{mAh/g}$ ). This is consistent with previous study that showed that an alloy with similar composition ( $\text{La}_{0.7}\text{Mg}_{0.3}\text{Al}_{0.2}\text{Mn}_{0.1}\text{Co}_{0.75}\text{Ni}_{2.45}$ ) exhibited a maximum discharge capacity of 340  $\text{mAh/g}$  [13].

**Table 3.** Charge capacity, discharge current density and specific discharge capacity for the Ni-MH battery prepared with a negative electrode using the  $\text{La}_{0.7}\text{Mg}_{0.3}\text{Al}_{0.3}\text{Mn}_{0.4}\text{Co}_{0.5}\text{Ni}_{3.8}$  alloy.

Cycle	Charge capacity (mAh)*	Charge current (mA $\text{g}^{-1}$ )	Discharge current (mA $\text{g}^{-1}$ )	Discharge time (h)	Specific capacity (mAh $\text{g}^{-1}$ )	<i>n</i> H atoms per unit cell
1	200	2857	173	1.25	178	2.57
2	200	2857	173	1.30	185	2.67
3	100	1429	173	2.23	319	4.61
4	50	714	173	2.45	350	5.05
5	30	429	173	2.33	333	4.81
6	40	571	173	2.40	343	4.95
7	60	857	173	2.48	354	5.11
8	80	1143	173	2.45	351	5.07
9	100	1429	173	2.26	323	4.66
10	50	714	173	2.37	339	4.89
11	50	714	286	0.85	243	3.51
12	50	714	214	1.22	261	3.77
13	50	714	173	2.10	300	4.33
14	50	714	71	4.80	343	4.95
15	50	714	173	1.63	233	3.36
16	50**	286	173	1.80	257	3.71

• Charged for 1h; \*\* 20 mA for 2.5 h

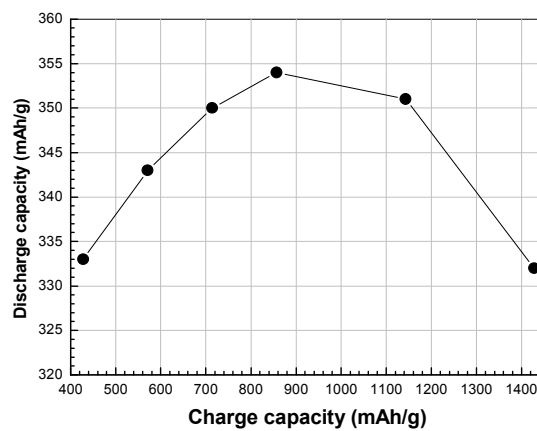


**Fig. 4 -** Specific charge capacity versus specific discharge capacity of the battery prepared with the  $\text{La}_{0.7}\text{Mg}_{0.3}\text{Al}_{0.3}\text{Mn}_{0.4}\text{Co}_{0.5}\text{Ni}_{3.8}$  alloy.

Fig. 5 shows the charge capacity density versus efficiency of this alloy. An efficiency of about 50% is achieved by using a charge capacity approximately  $700 \text{ mAhg}^{-1}$ . The discharge curve for this La-based battery charged at high rate is shown in Fig. 6a. There is a rapid drop in the voltage followed by a recovery in the curve. This behavior is similar to that found in lead acid batteries and known as the 'coup de fouet' phenomenon, attributed to a problem with the internal resistance of the battery. This behavior has not been reported for Ni-MH batteries and has been attributed to the excessively high charging rate used in this second cycle to activate the negative electrode. This effect was not observed in the subsequent cycles with lower charging rates. The discharge curve for the fourth cycle for the La-based battery is shown in Fig. 6b. A normal behavior can be observed in this case. The fast decrease in the electrode capacity with cycling was attributed to the fast activation with high charging rates and also to crushing and handling the alloy in air.

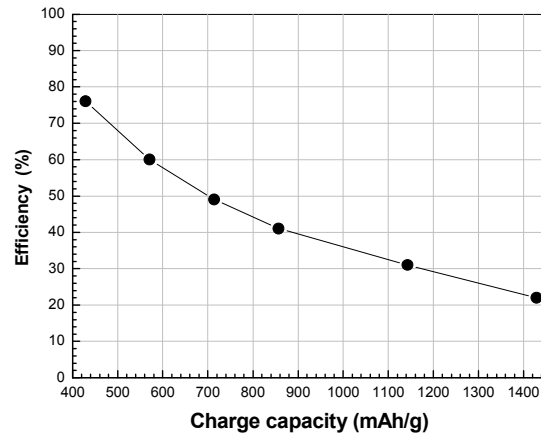


**Fig. 5** - Charge capacity versus efficiency of the battery prepared with the  $\text{La}_{0.7}\text{Mg}_{0.3}\text{Al}_{0.3}\text{Mn}_{0.4}\text{Co}_{0.5}\text{Ni}_{3.8}$  alloy.

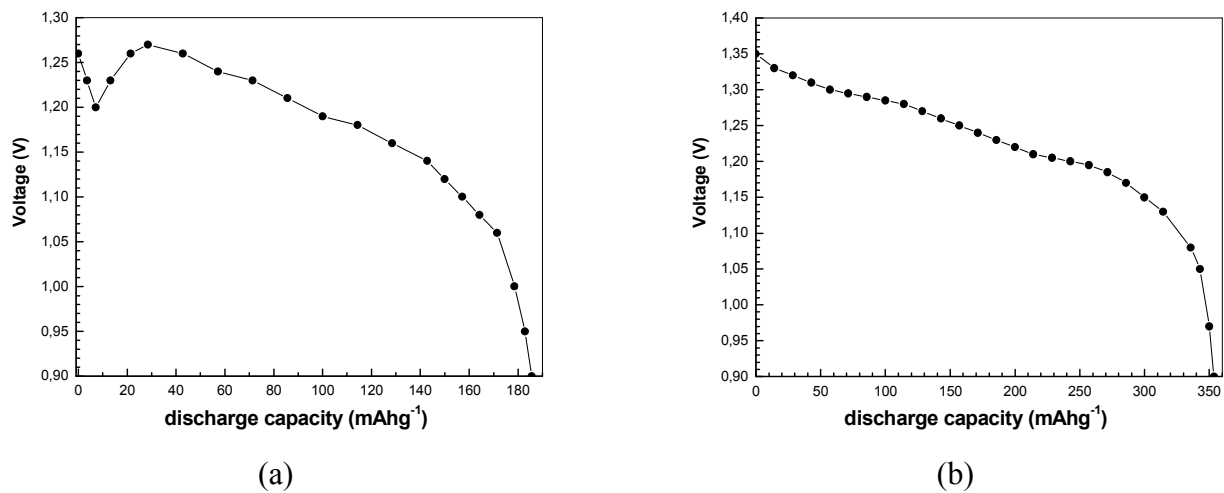


**Fig. 6** - Discharge curves for the La-based battery: a) second cycle and b) fourth cycle.

## Conclusions

The negative electrode, produced with a  $\text{La}_{0.7}\text{Mg}_{0.3}\text{Al}_{0.3}\text{Mn}_{0.4}\text{Co}_{0.5}\text{Ni}_{3.8}$  cast alloy, exhibited an excellent performance and a maximum discharge capacity of 354 mAh/g (at a discharge density of  $173 \text{ mA g}^{-1}$ ). An efficiency of  $\sim 50\%$  is achieved by using a charge capacity of about  $700 \text{ mAh g}^{-1}$ . The negative electrode was fast activating to the maximum capacity by charging at very high rate. The fast decrease in the electrode capacity with cycling was attributed to this fast activation using high charging rates and also by crushing and handling the alloy in air.

## Acknowledgements

The authors wish to thank FAPESP, CAPES and IPEN-CNEN/SP for the financial support and infrastructure made available to carry out this investigation. Thanks are due to J. C. S. Casini for the assistance in this work.

## References

- [1] F. Feng, M. Geng and D. O. Northwood: International Journal of Hydrogen Energy Vol. 26 (2001), p.725.
- [2] A. K. Shukla, S. Venugopalan and B. Hariprakash: Journal of Power Sources Vol.100 (2001), p. 125.
- [3] K. Hong: Journal of Alloys and Compounds Vol. 321 (2001), p. 307.

- [4] R. C. Ambrosio and E. A. Ticianelli: *Journal of Power Sources* Vol. 110 (2002), p. 73.
- [5] I. P. Jain and M. I. S. Abu Dakka: *International Journal of Hydrogen Energy* Vol. 27 (2002), p. 395.
- [6] H. Ye, Y. X. Huang, T. S. Huang and H. Zhang: *Journal of Alloys and Compounds* Vol. 330-332 (2002), p. 866.
- [7] Y. Liu, H. Pan, M. Gao, Y. Zhu, Y. Lei and Q. Wang: *International Journal of Hydrogen Energy* Vol. 29 (2004), p. 297.
- [8] H. Pan, Q. Jin, M. Gao, Y. Liu, R. Li and Y. Lei: *Journal of Alloys and Compounds* Vol. 373 (2004), p. 237.
- [9] H. Pan, X. Wu, M. Gao, N. Chen, Y. Yue and Y. Lei: *International Journal of Hydrogen Energy*, Vol. 31 (2006), p. 517.
- [10] T. Ozaki, H. B. Yang, T. Iwaki, S. Tanase, T. Sakai, H. Fukunaga, N. Matsumoto, Y. Katayama, T. Tanaka, T. Kishimoto and M. Kuzuhara: *Journal of Alloys and Compounds* Vol. 408-412 (2006), p. 294.
- [11] J. Hongmei, L. Guoxun, Z. Chuanhua and W. Ruikun: *J. Power Sources* Vol. 77 (1999), p.123.
- [12] K. Kadir, D. Noreus and I. Yamashita: *J. Alloys and Comp.* Vol. 345 (1-2) (2002), p. 140.
- [13] H. Pan, N. Chen, M. Gao, R. Li, Y. Lei and Q. Wang: *J. Alloys and Comp.* Vol. 397 (1-2) (2005), p. 306.
- [14] Y. F. Liu, H. G. Pan, R. Li and Y. Q. Lei: *Materials Science Forum* Vol. 473-470 (2005), p. 2457.

## **Advanced Powder Technology VII**

doi:10.4028/www.scientific.net/MSF.660-661

## **The Effect of High Charging Rates Activation on the Specific Discharge Capacity and Efficiency of a Negative Electrode Based on a LaMgAlMnCoNi Alloy**

doi:10.4028/www.scientific.net/MSF.660-661.133